Particle Size and Monomer Partitioning in Microemulsion Polymerization. 1. Calculation of the Particle Size Distribution

John D. Morgan and Eric W. Kaler*

Center for Molecular and Engineering Thermodynamics, Department of Chemical Engineering, University of Delaware, Newark, Delaware 19716

Received November 21, 1997; Revised Manuscript Received March 2, 1998

ABSTRACT: Exact analytical expressions are derived for the particle size and molecular weight distributions formed in microemulsion polymerization. These results follow directly from a mechanistic model of the polymerization reaction which has been quantitatively validated in kinetic studies. An additional mild assumption regarding radical exit is necessary, and it is assumed there is no particle coalescence. The theoretical distributions are used to simulate results from quasielastic light scattering and gel permeation chomatography. The shape of the predicted particle size distributions and the effect of initiator concentration, microemulsion composition, and conversion on the average particle size all agree with experiment.

1. Introduction

Microemulsion polymerizations are an interesting class of compartmentalized polymerization reactions that show distinct mechanistic differences from classical emulsion polymerization. Microemulsions are thermodynamically stable one-phase self-assembled solutions containing surfactant, oil, and water. The fundamental processes governing the reaction kinetics and latex properties in microemulsion polymerization have been investigated in a number of studies.[1−13] Most of this work has been interpreted at a qualitative level, although some attempts to quantify the reaction kinetics have been made.[9,10,12] We have recently described the polymerization kinetics of hexyl methacrylate (C_6MA) in microemulsions prepared with a mixture of the surfactants dodecyltrimethylammonium bromide and didodecyldimethylammonium bromide (DTAB and DDAB, respectively).[12] This system obeys very simple kinetics, and algebraic expressions derived from a mechanistic model are available for the conversion and reaction rate as a function of time. The theory is in quantitative agreement with experimental data, providing a high degree of confidence in the underlying assumptions.

The aim of a mechanistic model is primarily to allow prediction and control of the polymer and latex properties. The model developed in the kinetic analysis of the C_6MA polymerization also leads directly to a theory for the particle size and molecular weight distributions (PSD and MWD), which we describe in this article. The results can again be expressed in closed form and relate the distribution functions to the microemulsion composition and initiator concentration. An alternative approach based on surfactant packing has been described.[3,4,14] However, such an approach makes no allowance for growth of the microemulsion droplets beyond their initial unpolymerized size.

Given the distribution functions one may calculate the various moments reported by techniques such as quasielastic light scattering (QLS) and gel permeation chromatography (GPC), allowing experimental tests of the theory. Predictions of the number of chains per particle may also be made, which allow for experimental tests of the extent of radical exit from particles. The distributions calculated here are also used in the interpretation of the small angle neutron scattering (SANS) experiments described in the accompanying paper.

2. Derivation of the Particle Size Distribution

The reaction kinetics of the C_6MA O/W microemulsion polymerization system initiated with aqueous V-50 or buffered potassium persulfate have been analyzed elsewhere, resulting in a simple model that accurately describes the observed reaction rates, which we summarize here.[12] The most important mechanistic differences between microemulsion and emulsion polymerizations are the absence of a dispersed monomer phase, particle nucleation throughout the reaction, and the absence of termination. Radicals generated by initiator decomposition in the aqueous phase initiate polymerization in monomer-swollen micelles ("droplets"). Termination can be neglected, which leaves as the important processes radical production, propagation, monomer partitioning, and chain transfer reactions. The rate of radical production is determined by the rate of initiator decomposition, which can be taken as constant on the time scale of the reaction. Therefore the concentration of radicals in the microemulsion N^* is simply

$$N^* = \rho_o t \tag{1}$$

with the rate of radical production, ρ_o given by

$$\rho_o = 2k_d[\mathrm{I}] \tag{2}$$

where k_d is the initiator decomposition rate constant with units of M^{-1} s^{-1} and [I] is the initiator concentration in moles per liter of microemulsion. These expressions reflect the assumptions of no termination, fast entry of radicals into particles, and 100% initiator efficiency and have been justified elsewhere. Transfer reactions have no effect on N^* under these assumptions as transfer-generated monomeric radicals are assumed

* To whom correspondence should be addressed.

S0024-9297(97)01717-8 CCC: $15.00
Published on Web 04/21/1998

to react rapidly with available monomer without termination, and so continue propagating.

The rate at which these radicals propagate is proportional to the monomer concentration at the locus of polymerization, c. The SANS experiments described in the following paper have confirmed independent of the present analysis that the monomer is retained by the microemulsion droplets rather than swelling the polymer particles and that propagation occurs in the palisade layer—the monomer-saturated surfactant monolayer at the particle surface. The value of c can be calculated by assuming that monomer is dissolved in the hydrocarbon chains of the surfactant and that the palisade layer is in equilibrium with the monomer-swollen droplets. Therefore c is proportional to the amount of unreacted monomer in the microemulsion, or

$$c = c_o(1 - f) \tag{3}$$

giving the propagation rate of a single chain as

$$\frac{\partial L}{\partial t} = k_p c_o(1 - f) \tag{4}$$

where L is the length of the chain in monomer units, k_p is the propagation rate constant, f is the fractional conversion and c_o is an initial concentration of monomer equal to the concentration in a droplet of the unpolymerized microemulsion. The overall rate of polymerization is therefore

$$\frac{\partial f}{\partial t} = At(1 - f) \tag{5}$$

where A is a constant bundle

$$A = \frac{\rho_o k_p c_o}{M_o} \tag{6}$$

and M_o is the bulk concentration of monomer in moles per liter of the original microemulsion. Solution of eq 5 gives

$$f = 1 - \exp\left(-\frac{1}{2}At^2\right) \tag{7}$$

This straightforward analysis has been experimentally validated. We now use it to develop expressions for the particle size and molecular weight distributions. This requires the introduction of one further element to the model—the treatment of radical transfer reactions and the exit of monomeric free radicals. We will calculate the distribution functions in each of two limiting cases—(1) no radical exit events and (2) transfer-controlled exit. In each case it is assumed that there is no particle coalescence. This is reasonable given the high concentration of surfactant in the microemulsion. Practically, polymerized microemulsions have been observed to be very stable, and the absence of kinetically observable consequences of termination suggests coalescence is negligible.[12]

Case 1. No Exit. In this case we assume that any monomeric radicals generated by chain transfer do not exit but continue propagating in the same particle. We define the kinetic chain length as the length of polymer chain in monomer units resulting from propagation from a single radical, ignoring breaks in the physical chain due to chain transfer. Consider the function $L(t_1,t)$, the kinetic chain length at time t of a chain that was initiated at time t_1. This is simply the integral of the propagation rate (equation 4) using the expression for f of eq 7

$$L(t_1,t) = \int_{t_1}^{t} c_o \exp\left(-\frac{1}{2}At'^2\right) dt' \tag{8}$$

$$= L_\infty\left\{\operatorname{erf}\sqrt{\frac{A}{2}}t - \operatorname{erf}\sqrt{\frac{A}{2}}t_1\right\} \tag{9}$$

where $\operatorname{erf}(x)$ is the error function and L_∞ is the length of the longest possible chain, *i.e.*, $L(0,\infty)$, with the value

$$L_\infty = k_p c_o\sqrt{\frac{\pi}{2A}} \tag{10}$$

We may alternatively express this result as $t_1(L,t)$, the time at which initiation must occur in order for a chain to reach a kinetic length L at time t

$$t_1(L,t) = \sqrt{\frac{2}{A}}\operatorname{inverf}\left\{\operatorname{erf}\sqrt{\frac{A}{2}}t - \frac{L}{L_\infty}\right\} \tag{11}$$

where $\operatorname{inverf}(x)$ is the inverse of the error function.

To calculate the distribution of kinetic chain lengths at time t, we need to specify the number of chains of given length that were initiated at the earlier time $t_1(L,t)$. This is given by

$$n_L(L,t) = \rho_o\tau(t_1(L,t)) \tag{12}$$

where $\tau(t_1)$ is the average time between propagation events at time t_1. n_L has units of concentration. The rationale for this expression is that any entry event occurring within the time window defined by $t_1 \pm {}^1/_2\tau$ results in a chain of kinetic length L at time t. $\tau(t_1)$ is simply the inverse of the propagation rate at time t_1, or

$$\tau(t_1) = \frac{1}{k_p c_o}\exp\left(\frac{1}{2}At_1^2\right) \tag{13}$$

Since no termination could be discerned in the kinetic experiments, we ignore the possibility of more than one entry event occurring per particle. This is quite reasonable given that the number of microemulsion droplets present at any time outnumbers the number of particles by a factor of at least 1000,[6,11] so radicals will almost exclusively enter uninitiated droplets.

Substituting eqs 10, 11 and 13 into eq 12 gives the distribution of kinetic chain lengths at time t:

$$n_L(L,t) = \frac{\rho_o}{k_p c_o}\exp\left[\left(\operatorname{inverf}\left\{\operatorname{erf}\sqrt{\frac{A}{2}}t - \frac{L}{L_\infty}\right\}\right)^2\right] \tag{14}$$

This distribution function is defined in the usual manner, i.e., $n_L(L,t)\,dL$ is the concentration of particles containing chains with kinetic lengths between L and $L + dL$. This is converted into a size distribution by noting that

$$\frac{L}{L_\infty} = \left(\frac{r}{r_\infty}\right)^3 \tag{15}$$

$$dL = 3L_\infty r_\infty^{-3} r^2\,dr \tag{16}$$

where r is the particle radius and r_∞ the radius of the largest possible particle. r_∞ is related to L_∞ as

$$r_\infty = \left(\frac{3M_w L_\infty}{4\pi\rho_{poly}N_A}\right)^{1/3} \tag{17}$$

where M_w is the monomer molecular weight, ρ_{poly} is the polymer density, and N_A is Avogadro's number. The time (or equivalently conversion) dependent particle size distribution under the no exit, no termination assumptions, is then

$$n_r(r,t) = 3L_\infty r_\infty^{-3}\frac{\rho_o}{k_p c_o}r^2 \exp\left[\left(\text{inverf}\left\{\text{erf}\sqrt{\frac{A}{2}}t - \left(\frac{r}{r_\infty}\right)^3\right\}\right)^2\right] \tag{18}$$

where $n_r(r,t)\,dr$ is the concentration of particles with radii in the range r to $r + dr$.

Case 2. Transfer-Controlled Exit. The rate of transfer of free radical activity from a propagating chain to monomer is $k_{tr}c$, where k_{tr} is the transfer rate constant. Chain transfer results in a dead chain and a monomeric radical. The radical may continue to propagate in the original particle (as assumed in case 1). Alternatively, it may pass to another particle or droplet by exit to the aqueous phase followed by re-entry or by a coalescence−decoalescence event in which surfactant and monomer are exchanged between the coalescing species. Whether the radical propagates in the same or a different particle is determined by the time scales of these various events. To propagate within the original particle, the time scale of propagation, typically on the order of 10^{-3} s, must be shorter than either the time scale of monomer diffusion within the particle or the time scale of a coalescence event. The time scale for diffusion across a 20 nm radius particle is on the order of 10^{-6} s for a diffusion coefficient of 10^{-5} cm^2 s^{-1}, much shorter than the propagation time scale. The time scale of droplet coalescence in microemulsions has been reported to be on the order of 10^{-6} s. Therefore, the probable fate of a transfer-generated radical is exit and re-entry. In emulsion polymerization, radical exit is known to be the most likely event for small particles, even for quite hydrophobic monomers such as styrene,[15] and we presume it to be the case here. Consequently, the rate of radical exit is taken to be $k_{tr}c$. Again, we assume only one entry event per particle and thus one chain per particle.

Calculation of the PSD in this case proceeds in a manner similar to case 1. Equation 12 must be modified to include the rate of initiation by transfer-generated radicals, in addition to initiation by primary initiator radicals. The overall rate of entry is $\rho_o + k_{tr}cN^*$, or

$$\rho(t_1) = \rho_o\left(1 + k_{tr}c_o t_1 \exp\left(-\frac{1}{2}At_1^2\right)\right) \tag{19}$$

There are two ways a chain of length L may be found at time t: the chain may be a growing chain initiated at an earlier time $t_1(L,t)$ which has not undergone a transfer reaction, or it may be a dead chain that was initiated at some time prior to t_1 which underwent transfer at a length L. The distribution function is therefore constructed as

$$n_L(L,t) = \rho(t_1)\tau(t_1)P_{live}(L) + \int_0^{t_1}\rho(t'_1)\,dt'_1\,P_{dead}(L) \tag{20}$$

with $t_1(L,t)$ given by eq 11. $P_{live}(L)$ is the probability that a growing chain reaches a length L without undergoing transfer, and $P_{dead}(L)$ is the probability that the chain undergoes transfer at a length L. P_{dead} is simply the normalized transfer-limited molecular weight distribution function:[15]

$$P_{dead}(L) = \frac{k_{tr}}{k_p}\exp\left(-\frac{k_{tr}}{k_p}L\right) \tag{21}$$

P_{live} may be written as

$$P_{live}(L) = 1 - \int_0^L P_{dead}(L')\,dL' \tag{22}$$

so

$$P_{live}(L) = \exp\left(-\frac{k_{tr}}{k_p}L\right) \tag{23}$$

Substitution of eqs 19, 21 and 23 into eq 20 yields the transfer-controlled molecular weight distribution. The integral in eq 20 is readily evaluated to obtain an expression in closed form, a result which is most compactly expressed as

$$n_L(L,t) = \frac{\rho_o d}{k_p c_o b}(1 + abL_L) + \frac{\rho_o k_{tr}}{k_p}\frac{d}{\sqrt{2A}}(2\Lambda_L + a(1-b)) \tag{24}$$

where

$$\Lambda_L = \text{inverf}\left(\text{erf}\left(\sqrt{\frac{A}{2}}t\right) - \left(\frac{L}{L_\infty}\right)\right) \tag{25}$$

$$a = k_{tr}c_o\sqrt{\frac{2}{A}} \tag{26}$$

$$b = \exp(-\Lambda_L^2) \tag{27}$$

$$d = \exp\left(-\frac{k_{tr}}{k_p}L\right) \tag{28}$$

Since the assumptions imply only one chain per particle, eq 24 may equivalently be expressed as the particle size distribution by effecting the change of variables suggested by eqs 15 and 16

$$n_r(r,t) = 3L_\infty r_\infty^{-3}r^2 \times \left[\frac{\rho_o d}{k_p c_o b}(1 + ab\Lambda_r) + \frac{\rho_o k_{tr}}{k_p}\frac{d}{\sqrt{2A}}(2\Lambda_r + a(1-b))\right] \tag{29}$$

where

$$\Lambda_r = \text{inverf}\left(\text{erf}\left(\sqrt{\frac{A}{2}}t\right) - \left(\frac{r}{r_\infty}\right)^3\right) \tag{30}$$

This result satisfies appropriate limits and mass balance criteria. In the limit of no exit ($k_{tr} = 0$), these results collapse to the case 1 solutions. The mass balance on polymer

$$\int_0^\infty L\, n_L(L,f)\, \mathrm{d}L = fM_o \tag{31}$$

the particle volume balance

$$\int_0^\infty \frac{4}{3}\pi r^3 n_r(r,f)\, \mathrm{d}r = \frac{fM_oM_w}{N_A\rho_{poly}} \tag{32}$$

the number balance on particles calculated from n_L

$$\int_0^\infty n_L(L,t)\, \mathrm{d}L = \rho_o\int_0^t 1 + k_{tr}c_o t' \quad \exp\left(-\frac{1}{2}At'^2\right) \mathrm{d}t' \tag{33}$$

and n_r

$$\int_0^\infty n_r(r,t)\, \mathrm{d}r = \rho_o t + \frac{\rho_o k_{tr} c_o}{A}\left(1 - \exp\left(-\frac{1}{2}At^2\right)\right) \tag{34}$$

are all satisfied, as confirmed by numerical integration of n_L and n_r (the expressions on the right-hand side of eqs 33 and 34 are identical).

3. Observables in the QLS Experiment

The most reliable method for obtaining experimental PSDs is electron microscopy, although artifacts can influence the results. Given the convenience of QLS, however, it is worthwhile to consider how the theoretical distributions would appear in terms of the average radii and polydispersities reported by a QLS experiment. We will therefore briefly outline the theory of the QLS experiment[16] and calculate the experimental observables using the theoretical distributions.

A homodyne experiment measures the reduced first-order intensity autocorrelation function $g^{(1)}(\tau)$. For a polydisperse sample, the function $g^{(1)}(\tau)$ is composed of a spectrum of decay times corresponding to each size component present in the sample, weighted by $G(\Gamma)$, the normalized intensity of light scattered by each size component

$$g^{(1)}(\tau) = \int_0^\infty G(\Gamma)\mathrm{e}^{-\tau\Gamma}\, \mathrm{d}\Gamma \tag{35}$$

with

$$\int_0^\infty G(\Gamma)\, \mathrm{d}\Gamma = 1 \tag{36}$$

$\Gamma = Dq^2$, where D is the diffusion coefficient and q is the magnitude of the scattering vector. The Laplace transform in eq 35 can be expanded to give

$$\ln g^{(1)}(\tau) = \langle\Gamma\rangle\tau + \frac{\mu_2}{2!}\tau^2 - \ldots \tag{37}$$

where μ_2 is the variance

$$\mu_2 = \frac{\langle\Gamma^2\rangle - \langle\Gamma\rangle^2}{\langle\Gamma\rangle^2} \tag{38}$$

and the moments are defined by

$$\langle\Gamma^i\rangle = \int_0^\infty \Gamma^i G(\Gamma)\, \mathrm{d}\Gamma \tag{39}$$

$\langle\Gamma\rangle$ and μ_2 are obtained from $g^{(1)}(\tau)$ using eq 37. From $\langle\Gamma\rangle$ is obtained the intensity weighted diffusion coefficient $\langle D\rangle$, which is proportional to $\langle r^{-1}\rangle$. Therefore the radius reported by the QLS experiment, $\langle r\rangle_{qls}$, is $\langle r^{-1}\rangle^{-1}$.

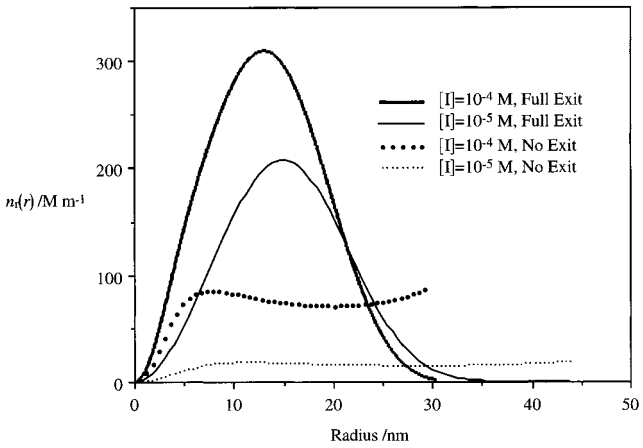

Figure 1. Particle size distribution at 98% conversion calculated for the no exit (eq 18) and full exit (eq 29) cases at two initiator concentrations. Parameter values are $c_o = 1.8$ M, $k_d = 2 \times 10^{-5}$ M^{-1} s^{-1}, $k_p = 995$ M^{-1} s^{-1}, $M_o = 0.257$ M, and $k_{tr} = 0.01$ M^{-1} s^{-1}.

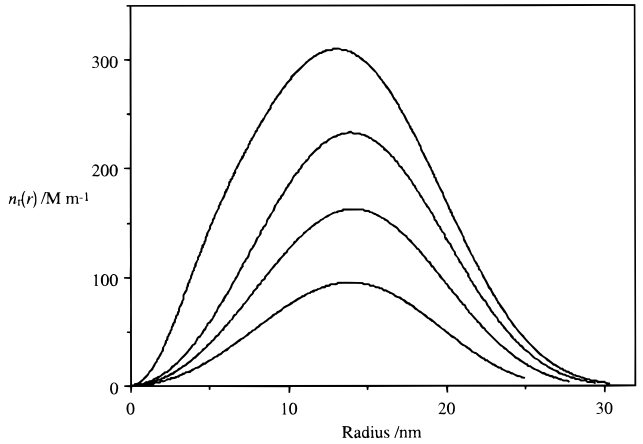

Figure 2. Evolution of the particle size distribution with conversion in the case of full exit. From bottom to top: 25%, 50%, 75%, and 98% conversion. [I] = 10^{-4} M, $k_{tr} = 0.01$ M^{-1} s^{-1}, and other values are as for Figure 1.

To calculate $\langle r\rangle_{qls}$ and μ_2 from the distribution function of eq 29, note that[17]

$$G(\Gamma(q,r)) = n_r(r)V^2P(q,r) \tag{40}$$

to within an arbitrary normalization constant, where V is the volume of the sphere and P is the form factor of a sphere

$$P(q,r) = \left[\frac{3}{q^3r^3}(\sin(qr) - qr\cos(qr))\right]^2 \tag{41}$$

Constant factors cancel, and

$$\langle r(t)\rangle_{qls} = \frac{\int_0^\infty r^6P(q,r)n_r(r,t)\, \mathrm{d}r}{\int_0^\infty r^5P(q,r)n_r(r,t)\, \mathrm{d}r} \tag{42}$$

μ_2 is found using eq 40 in the calculation of the moments of eq 38.

4. Predicted Distributions and Properties

Figures 1 and 2 show particle size distributions for the exit and no exit cases using values for the kinetic parameters (given in the figure caption) appropriate for

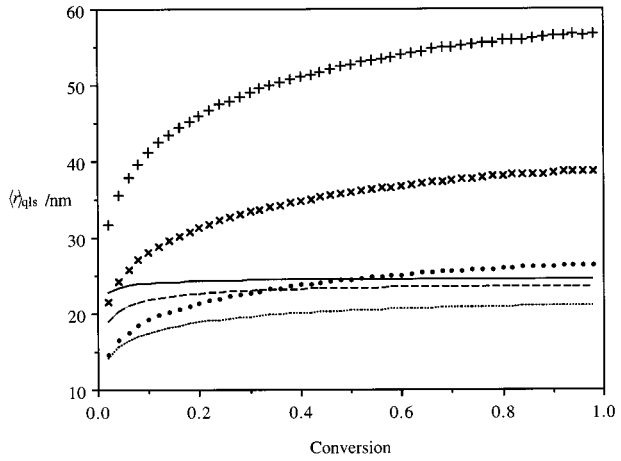

Figure 3. QLS radius vs conversion at different initiator concentrations. For full exit ($k_{tr} = 0.01$ M^{-1} s^{-1}): solid line, [I] $= 10^{-6}$ M; dashed line, [I] $= 10^{-5}$ M; dotted line, [I] $= 10^{-4}$ M. For no exit: +, [I] $= 10^{-6}$ M; ×, [I] $= 10^{-5}$ M; ●, [I] $= 10^{-4}$ M. Other values are as for Figure 1.

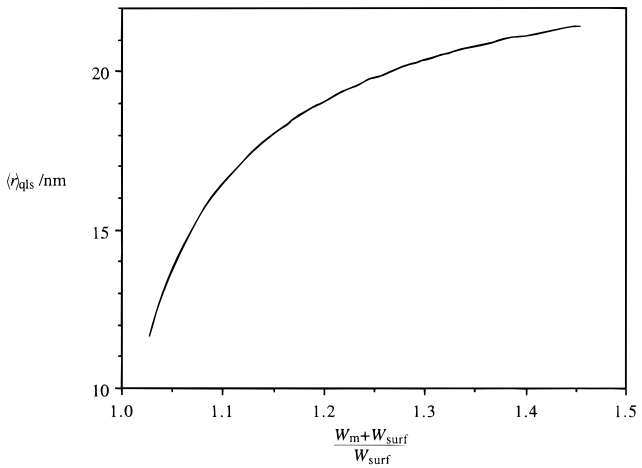

Figure 4. QLS radius for the full exit case at 98% conversion as a function of initial microemulsion composition, expressed in Antonietti and Wu's form.[4] [I] $= 10^{-4}$ M, $k_{tr} = 0.01$ M^{-1} s^{-1}, and other parameters are as for Figure 1.

the microemulsion polymerization of C_6MA under the experimental conditions in our kinetic study.[12] k_{tr} has not been measured for this monomer. For the purposes of calculation, we assume a value of $k_{tr} = 0.01$ M^{-1} s^{-1}, which is of a similar magnitude to transfer constants reported for other alkyl methacrylates.[18] The particle sizes range up to about 35 nm, which is typical of the many reports of the particle size obtained in experimental studies.[2,4]

Figure 1 compares the full exit and no exit cases at different initiator concentrations at 98% conversion. In the no exit case the distribution has two weak maxima. The finite number of large particles is an expected consequence of denied exit. The peak at smaller size only appears late in the reaction, above 90% conversion, and is a consequence of a constant rate of particle creation at a time when the propagation rate is approaching zero. Many new particles are formed but their growth rate is limited because of the low monomer concentration. In the case of full exit the distribution is monomodal and nearly symmetric as the particle size is largely controlled by chain transfer. The median size is not strongly affected by the initiator concentration or extent of reaction (Figure 2).

The full exit distributions are in qualitative agreement with the distributions obtained by electron microscopy for the microemulsion polymerization of styrene initiated with persulfate[8,9] and methyl methacrylate (MMA) initiated with V-50.[19] These distributions are of the same shape as calculated here, and show little change with conversion. They effectively refute the possibility of no exit in the case of these monomers since n_r approaches zero for large sizes. It seems likely that full exit should also hold for C_6MA, although this cannot be stated with certainty due to the lower aqueous solubility of C_6MA. It should be noted that the kinetics of polymerization in the persulfate-initiated styrene system deviate from the kinetics assumed here, due possibly to an initiator artifact.[12] However, a qualitative comparison is still permissible. The kinetics of the MMA system appear to be very similar to the C_6MA kinetics.

The QLS radii calculated from the distributions are shown in Figure 3 as a function of conversion for the exit and no exit cases at different initiator concentrations. $\langle r \rangle_{qls}$ increases as the initiator concentration is decreased. This trend has been reported in experimental studies, and is a consequence of the slower reaction rate at lower initiator concentrations which allows more time for particle growth and the development of the high molecular weight tail of the MWD. The effect is quite pronounced for the case of no exit. In the case of full exit $\langle r \rangle_{qls}$ is virtually independent of conversion. This has been observed for microemulsion polymerization of styrene.[6] The distributions have polydispersities of $\mu_2 \sim 0.04-0.08$, typical of experimental results.[6,11]

Figure 4 shows the effect on the QLS radius of varying the monomer-to-surfactant ratio in the initial microemulsion. The results are calculated for full exit at 98% conversion, and presented as a function of Antonietti and Wu's composition parameter $(W_m + W_{surf})/W_{surf}$, where W_m and W_{surf} are the weights of monomer and surfactant in the initial microemulsion.[4,14] To calculate this result c_o must be specified as a function of composition. We assumed the monomer to be solubilized in the hydrocarbon tails of the surfactant, giving

$$c_o = \frac{M_o V_o}{V_m + V_{chain}} \tag{43}$$

where V_o, V_m, and V_{chain} are the volumes of the whole microemulsion, the monomer and the volume associated with surfactant chains respectively, which are calculated assuming bulk values for the densities. c_o, M_o, W_m, and W_{surf} were calculated for the C_6MA/DTAB/DDAB/H_2O system for a constant surfactant content of 3.6 g/8.4 g DDAB/DTAB per 100 g of microemulsion while varying the C_6MA content.

The theory predicts an increase in particle size as the ratio of monomer to surfactant is increased. This has been observed for MMA and styrene over a small range of compositions.[7] The microemulsion polymerization of styrene in the presence of toluene shows an increase in particle size as styrene content is increased, which is also predicted by the theory.[8] Over a wider range of compositions, the geometric model of Antonietti and Wu predicts a linear plot for Figure 4, which is validated experimentally.[4] This is not the case for the present theory. However, most of the compositions examined by Antonietti and Wu fall outside the composition range shown in Figure 4 and outside the one-phase region reported for their monomer and surfactant system.[13] We

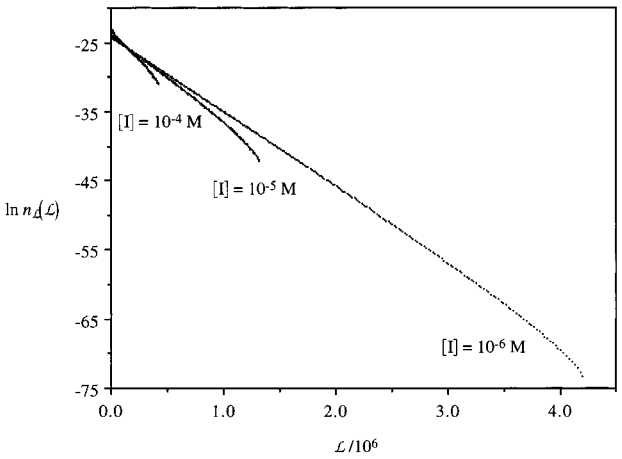

Figure 5. ln n_L vs L at 98% conversion for different initiator concentrations. $k_{tr} = 0.01$ M^{-1} s^{-1}, and other parameters are as for Figure 1.

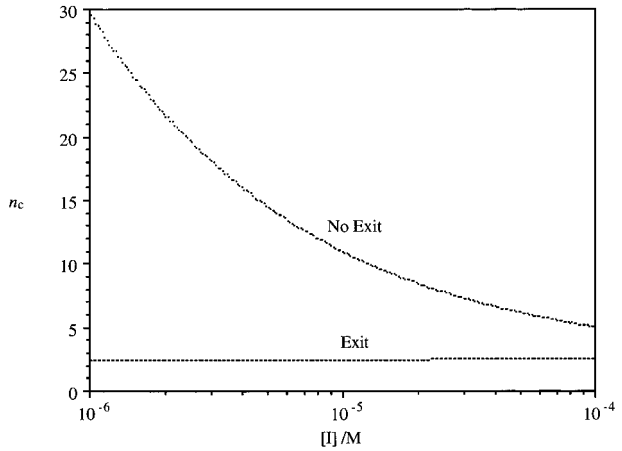

Figure 6. Number of chains per particle vs [I] for exit and no exit cases. n_c is calculated based on the number average molecular weight and the QLS average particle size. $k_{tr} = 0.01$ M^{-1} s^{-1}, and other parameters are as for Figure 1.

do not extend our predictions into the range they examined as our assumptions are not valid in a two-phase system.

Figure 5 shows the predicted molecular weight distributions at 98% conversion for several initiator concentrations. At low initiator concentrations the transfer-limited MWD (eq 21) is approached. At higher initiator concentrations deviations appear, and the slope of the ln n_L vs L plot is approximately double that of the transfer limited case. Larger chains appear at lower initiator concentrations due to the greater time available for chain growth.

Finally, the apparent number of chains per particle, n_c, can be calculated. This is normally obtained experimentally from the average molecular weight reported by GPC analysis and the average particle radius reported by QLS. In Figure 6 we plot n_c vs initiator concentration at 98% conversion based on the number average molecular weight and $\langle r \rangle_{qls}$. In the case of no exit, n_c follows approximately a power law decay, and a large number of chains per particle may appear at low intiator concentration. In the case of full exit the apparent value of n_c is approximately 2.5, independent of [I], despite the model strictly enforcing one chain per particle.

This apparent inconsistency is a result of calculating n_c by combining incommensurate measures of the chain length and particle size—in this case, the first moment of the MWD and the sixth moment of the PSD. As a consequence, the experimental reports that find several chains per particle are in fact consistent with just a single chain per particle. Reported experimental values for $n_c$may be found which agree with the full exit[6,8] or no exit[7] limits. The strong dependence of the apparent number of chains per particle on [I] in the no exit case compared to the case of full exit suggests a useful experimental test of the extent of exit in a given system.

5. Conclusions

Analytical expressions for the particle size and molecular weight distributions for microemulsion polymerization have been derived that follow directly from the same set of assumptions that have been successfully used in describing the reaction kinetics. An additional assumption regarding the degree of exit of transfer generated monomeric radicals is required. Alternatively, the predictions made here suggest several experimental tests for determining the extent of radical exit, in particular, the measurement of n_c as a function of initiator concentration. The shape of the distributions and the typical particle size agree with available experimental reports, and the dependences of the particle size on conversion, initiator concentration, and microemulsion composition are in qualitative agreement with experiments. Quantitative testing of these results in an appropriate experimental system is in progress.

References and Notes

(1) Candau, F.; Leong, Y. S.; Fitch, R. M. *J. Polym. Sci., Polym. Chem. Ed.* **1985**, *23*, 193.
(2) Candau, F. In *Polymerization in Organized Media*; C. M. Paleous, Ed.; Gordon and Breach Science Publisers: Philadelphia, PA, 1992; p 215.
(3) Antonietti, M.; Bremser, W.; Müschenborn, D.; Rosenauer, C.; Schupp, B.; Schmidt, M. *Macromolecules* **1991**, *24*, 6636.
(4) Antonietti, M. *Macromol. Chem. Phys.* **1995**, *196*, 441.
(5) Capek, I.; Potisk, P. *Macromol. Chem. Phys.* **1995**, *196*, 723.
(6) Full, A. P.; Kaler, E. W.; Puig, J. E.; Arellano, J. *Macromolecules* **1996**, *29*, 2764.
(7) Gan, L. M.; Lee, K. C.; Ng, S. C. *Langmuir* **1995**, *11*, 449.
(8) Guo, J. S.; El-Aasser, M. S.; Vanderhoff, J. W. *J. Polym. Sci., Polym. Chem.* **1989**, *27*, 691.
(9) Guo, J. S.; Sudol, E. D.; Vanderhoff, J. W.; El-Aasser, M. S. *J. Polym. Sci., Polym. Chem. Ed.* **1992**, *30*, 691.
(10) Guo, J. S.; Sudol, E. D.; Vanderhoff, J. W.; El-Aasser, M. S. *J. Polym. Sci., Polym. Chem. Ed.* **1992**, *30*, 703.
(11) Lusvardi, K. M., Ph.D. Thesis, University of Delaware, 1996.
(12) Morgan, J. D.; Lusvardi, K. M.; Kaler, E. W. *Macromolecules* **1997**, *30*, 1897.
(13) Pérez-Luna, V. H.; Puig, J. E.; Castaño, V. M.; Rodriguez, B. E.; Murthy, A. K.; Kaler, E. W. *Langmuir* **1990**, *6*, 1040.
(14) Wu, C. *Macromolecules* **1994**, *27*, 298.
(15) Gilbert, R. G. *Emulsion Polymerization*; Academic Press: London, 1995.
(16) Johnson, C. S.; Gabriel, D. A. *Laser Light Scattering*; Dover: New York, 1981.
(17) Guinier, A.; Fournet, G. *Small Angle Scattering of X-rays*; John Wiley & Sons: New York, 1955.
(18) *Polymer Handbook*; 3rd ed.; Brandrup, J., Immergut, E. H., Eds.; John Wiley & Sons: New York, 1989.
(19) Bléger, F.; Murthy, A. K.; Pla, F.; Kaler, E. W. *Macromolecules* **1994**, *27*, 2559.

MA971717I